

Josephson tunneling of a phase-im printed Bose-Einstein condensate in a time-dependent double-well potential

E. Sakellaris, N. P. Proukakis, M. Leadbeater, and C. S. Adams
Department of Physics, University of Durham, Durham DH1 3LE, United Kingdom

Abstract.

The direction of Josephson flow depends critically on the initial state of the system. This paper discusses the feasibility of experimental control of the flow direction of atomic Bose-Einstein condensates in a double-well potential using phase-imprinting. The flow is induced by the application of a time-dependent potential gradient, providing a clear signature of macroscopic quantum tunneling in atomic condensates. By studying both initial state preparation and subsequent tunneling dynamics we find the parameters to optimize the phase induced Josephson current. We find that the effect is largest for condensates of up to a few thousand atoms, and is only weakly-dependent on trap geometry.

^x To whom correspondence should be addressed (Eleni.Sakellaris@durham.ac.uk)

1. Introduction

The creation of superconducting [1] and super uid [2] weak links has led to the experimental observation of Josephson e ects [3], arising as a result of macroscopic quantum phase coherence. Josephson weak links are typically created by connecting two initially independent systems (superconductors / super uids) via a barrier with dimensions of the order of the system healing length. Such junctions lead to a variety of interesting phenomena [4], including dc- and ac-Josephson e ects. Observations in superconductors preceded those in super uids, due to the much larger healing lengths, thus enabling easier fabrication of weak links. Evidence for Josephson-like e ects has been observed in ^4He weak links [5], and unequivocally demonstrated for weakly-coupled ^3He systems [6]. The recent achievement of dilute trapped atomic Bose-Einstein condensation (BEC) [7] gives rise to a new system for studying Josephson e ects. In particular, such systems enable the investigation of dynamical regimes not easily accessible with other superconducting or super uid systems. The simplest atomic Josephson junction can be realized by a condensate con ned in a double-well potential. To allow control of the tunnelling rate, such a system can be constructed by raising a barrier within a harmonic trap containing an atomic condensate; this can be achieved by the application of a far-o -resonant blue-detuned laser beam, which induces a repulsive gaussian barrier [8]. Atomic interferometry based on such a set-up was recently reported [9]. Alternatively, a condensate can be created directly in a magnetic double-well structure [10]. Remarkable experimental progress has led to the creation of atomic BEC Josephson junction arrays, in which the harmonically trapped atoms are additionally con ned by an optical lattice potential, generated by far-detuned laser beams. Phase coherence in di erent wells was observed by interference experiments of condensates released from the lattice [11]. In addition, Josephson e ects [12] and the control of tunnelling rate have been demonstrated [14,13]. Although experiments (and theoretical analysis) of such systems are well underway, deeper insight into the diverse range of Josephson phenomena can be obtained by looking at the simplest single junction, double-well system. This system has already received considerable theoretical attention, with treatments based on a two-state approximation [15,16,17,18,19,20,21,22,23,24], zero temperature mean eld theory [25,26,27,29,30,28,31], quantum phase models [32,33] and instanton methods [34].

In this paper, we investigate the Josephson dynamics for a phase-imprinted atomic condensate in a double-well potential under the in uence of a time-dependent potential gradient. Imprinting a phase di erence of ϕ across the two wells induces atomic ow in the opposite direction to that of a condensate initially in its ground state. Such ow towards a region of higher potential energy provides a clear signature of Josephson tunnelling. This e ect is analogous to the behaviour across a superconducting -junction [35], in which the addition of a macroscopic phase di erence $\phi = \pi$ across the superconducting weak link leads to reversal of the sign of the current [36,37,38]. Note that a related e ect has been predicted for condensates in optical lattices as a result

of the renormalization of the mass in the lattice, based on Bloch wave analysis [39].

The superfluid analogue of a superconducting junction is a metastable state, recently observed in ^3He weak links [40]. Atom BEC junctions behave similarly to those of ^3He -B. Thus, although superconducting Josephson junctions can be mapped onto a rigid pendulum, atom condensate tunnel junctions map onto a non-rigid pendulum [19,17,18], thus exhibiting richer oscillation modes. For example, oscillations arise in such systems [19,17,18,20] with this effect already additionally discussed within the framework of an exact quantum phase model [33].

This paper is structured as follows. Sec. 2 introduces our main formalism, and introduces the low-lying states of a condensate in a double-well, while Sec. 3 discusses the dynamics associated with particular initial states under the addition of a time-dependent potential gradient. Under the action of a gradient, states with initial phase difference across them exhibit tunneling to the upper well, providing a clear manifestation of Josephson effects. The possibility of experimental observation of this phenomenon in current BEC set-ups is analysed in Sec. 4, with a short conclusion in Sec. 5.

2. Time-independent Properties of a BEC in a double-well potential

At low temperatures, the behaviour of a Bose-Einstein condensate is accurately described by a nonlinear Schrödinger equation known as the Gross-Pitaevskii (GP) equation. Throughout this paper we work in dimensionless (harmonic oscillator) units, by applying the following scalings: space coordinates transform according to $r_i^0 = a_?^{-1} r_i$, time $t^0 = !_? t$, condensate wavefunction $^0(r^0; t^0) = a_?^3 \psi(r; t)$ and energy $E^0 = (h !_?)^{-1} E$. Here $a_? = h = m !_?$ is the harmonic oscillator length in the transverse direction (s), where $!_?$ the corresponding trapping frequency. We thus obtain the following dimensionless GP equation (primes henceforth neglected for convenience) describing the evolution of the condensate wavefunction (normalized to unity)

$$i\partial_t \psi(r; t) = -\frac{1}{2} r^2 + V(r) + g j(r; t) \psi(r; t) : \quad (1)$$

The atom-atom interaction is parametrized by $g = g = (a_?^3 h !_?)$, where $g = N (4 \pi \hbar^2 a^3 m)$ is the usual three-dimensional scattering amplitude, defined in terms of the s-wave scattering length a , and N is the total number of atoms (mass m). The total confining potential (see Fig. 1(a)) is given by

$$V(r) = \frac{1}{2} [(x^2 + y^2) + z^2] + h \exp[-(z-w)^2] + z : \quad (2)$$

The first term describes a cylindrically symmetric harmonic trapping potential, with a trap aspect ratio $= !_z = !_?$: the trap is spherical for $= 1$, 'cigar-shaped' for < 1 and 'pancake-like' for > 1 . The second term describes a gaussian potential of height h generated by a blue detuned light sheet of beam waist w in the z direction, located at $z = 0$. In Eq. (2), the contribution z corresponds to an additional linear potential of gradient pivoted at the centre of the trap. For > 0 considered throughout this

paper, the right well obtains higher potential energy and the trap centre is additionally shifted into the $z > 0$ region; however, this shift is negligible for the parameters studied throughout this work, and will be henceforth ignored.

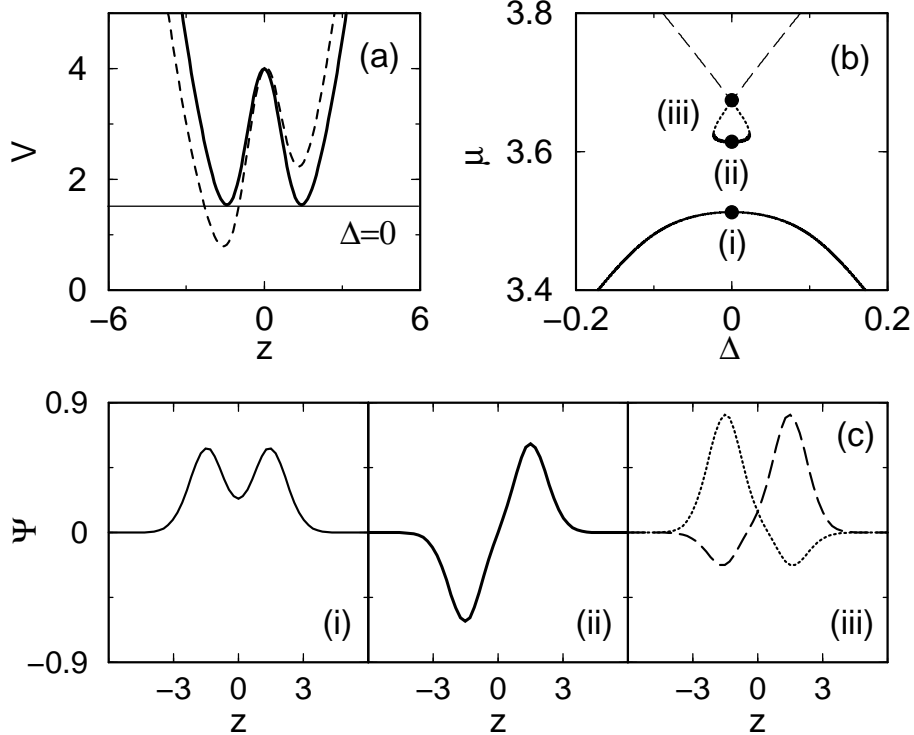


Figure 1. Double well potential with corresponding eigenenergies and eigenstates. (a) Schematic geometry of the total confining potential in the axial direction for a Gaussian barrier (height $h = 4h_1$, waist $w = a_1$) located at the centre of the trap. Plotted are the symmetric ($\ell = 0$, solid line) and asymmetric ($\ell = 0.5$, $h_1 = a_1$), dashed line) case. (b)–(c) Corresponding eigenenergies and eigenstates for the double-well as a function of the potential gradient: (i) ground state (lower solid line), (ii) anti-symmetric first-excited state with equal population in both wells (thick solid line), (iii) first excited state with unequal populations, having more population in left well (dotted), or in right well (dashed). Parameters used here are $g = 1$ and spherical trap geometry ($\ell = 1$).

The eigenstates of the double-well condensate are calculated by substituting $\Psi(r; t) = e^{i\omega t} \psi(r)$ and solving the resulting time-independent equation as discussed in [31]. As is well-known, sufficiently large interactions lead to the appearance of a loop structure, see e.g. [23, 41]. The loop structure for the first excited state is shown in Fig. 1(b). Corresponding wavefunctions for ground and first excited state are shown in Fig. 1(c) for $\ell = 0$. The three eigenstates are (i) a symmetric ground state with equal population in both wells, (ii) an anti-symmetric state with equal population in both wells and a phase difference of π across the trap centre, which we shall henceforth refer to as Ψ_e and (iii) two higher energy 'self-trapped' states with most of the population in either the left (dotted) or the right (dashed) well [16, 17, 18, 31]. This paper is mainly

concerned with states g and e and superpositions thereof. In particular, we will show that the dynamics of excited states in the presence of a time-dependent potential z are remarkably different to that of the ground state, and offer a clear demonstration of Josephson tunneling.

3. Tunneling dynamics under a time-dependent magnetic field gradient

The tunneling dynamics of an atomic condensate in a symmetric double-well ($\phi = 0$) are well-known [15,16,17,18,19,20,21,22,23,28]. If a system is initially prepared in one of its eigenstates, g or e , it will remain in that same state and there is no tunneling current. This is shown in Fig. 2(a) where we plot the fractional relative population, $N = (N_L - N_R)/(N_L + N_R)$ as a function of time with $\phi = 0$ for $t < 0$. However, if the system is prepared in a superposition of g or e , e.g.,

$$|\psi\rangle = \frac{1}{\sqrt{2}}(|g\rangle - |e\rangle); \quad (3)$$

the population tunnels back and forth, and the relative phase between the two wells oscillates around a mean value of π (anti-oscillations [19,17,18,20,33]). In this paper, we consider the tunneling of various initial states whose symmetry is further broken by the addition of a time-dependent potential gradient which increases linearly. The potential gradient is applied at $t = 0$, i.e., $\phi = Rt$ for $t > 0$, and, for $t > 0$, the right well lies higher than the left well (dashed line in Fig. 1(a)). The effect of the asymmetry is to induce a Josephson current to the left (lower potential energy region) for the initial state g , whereas flow occurs to the right (higher potential energy) for the state e (Fig. 2(a)). The observation of flow in opposite directions for suitably prepared initial states provides a very clear signature of macroscopic quantum tunnelling.

The situation is more complex for superposition states, such as $|\psi\rangle = \frac{1}{\sqrt{2}}(|g\rangle + |e\rangle)$. In this case, if the potential gradient is turned on rapidly (compared to the period of the anti-oscillations), the tunneling is immediately suppressed and the population is 'frozen' at its initial position. If the potential gradient is turned on more slowly, the oscillations between the wells continue with gradually decreasing amplitude, and there is a net flow to regions of higher potential, Fig. 2(b). However, the net flow to the higher potential well is smaller than in the case of $|e\rangle$. Also, the tunneling dynamics for $|g\rangle$ and $|\psi\rangle$ are different, i.e., the ensuing dynamics depends on the sign of the phase difference between the two wells, whereas such dependence is not encountered for $|e\rangle$. This difference can be used to distinguish between state $|e\rangle$ and superposition states in an experiment (see Section 4).

The tunneling behaviour of states g and e under a potential gradient can be explained in terms of the time-independent solutions [31]. These can be plotted as a function of time via their dependence on the time-dependent energy offset $\phi = Rt$ between the two wells. The time evolution and the corresponding time-independent population difference for state $|e\rangle$ is shown in Fig. 3(a), from which it is found that, for slow velocities, the system follows the eigenstate almost adiabatically.

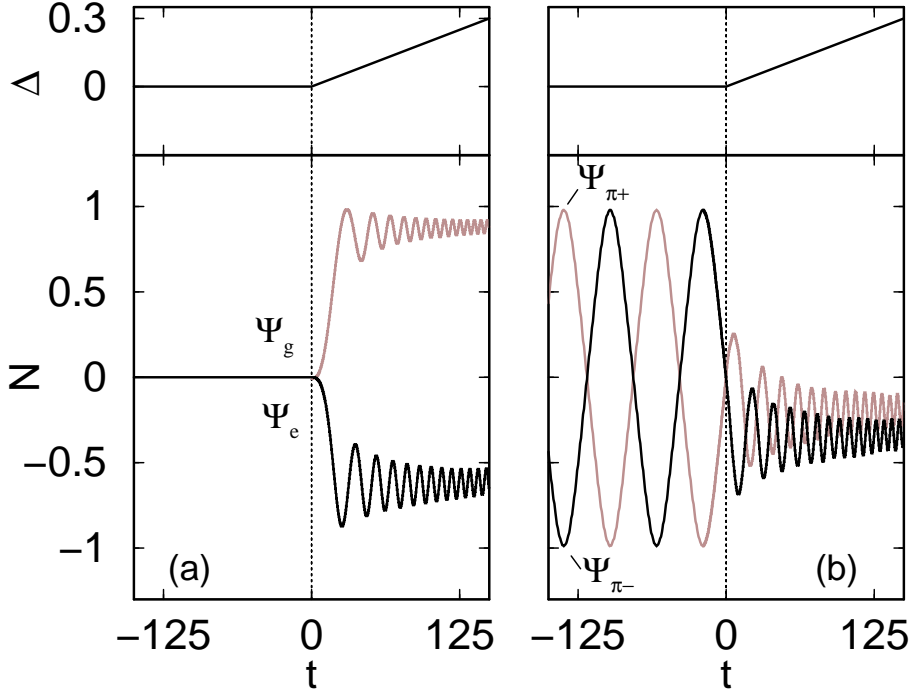


Figure 2. Evolution of fractional population difference N as a function of time t without ($t < 0$) and with ($t > 0$) a potential gradient $= R t$ (shown at the top of each figure) for different initial states: (a) a pure ground state $|\Psi_g\rangle$ or first excited state $|\Psi_e\rangle$ with equal populations in both wells. In this case, tunnelling only arises due to the additional external potential; (b) the superposition state $|\Psi_{\pi^+}\rangle - |\Psi_{\pi^-}\rangle$, showing clearly -oscillations for $t < 0$. The parameters used here are: $g = 1$, $h = 4h_?$, $R = 2 \times 10^{-3} (h_?)^2 = a_?$.

The initial dynamics discussed above is also well described by the two-state model [15,16,17,18,19,20,21,22,23,28] (grey line in Fig. 3(a)). However, for larger gradients the full potential GP calculation predicts that the atoms return to the lower (or left) potential well, as illustrated by the density snapshots in Fig. 3(b), whereas the two-state model suggests they remain in the upper (right) well. This breakdown of the two-state model occurs because it does not take higher lying modes into consideration [31]. This is an important consideration for any experimental demonstration of macroscopic flow to the higher well, as the two state model does not predict the important limitation on the experimental time scale for which the population remains in the higher well.

The flow towards the right (higher) potential well shown in Fig. 3(b) provides a clear macroscopic demonstration of quantum tunneling. To consider whether this effect is observable in current experimental set-ups, we have studied the effect of varying the nonlinearity, trap geometry, and the time dependence of the ramp. Note that the effect of interactions have also been considered in [27], with the effective interaction also modified by atom losses [42]. Our studies reveal that increasing the nonlinearity causes a reduction in the amount of initial flow to the upper well, and thus tends to inhibit the experimental observation (see next section for experimental estimates). For example, using the parameters of Fig. 3 with a nonlinearity ten times bigger (i.e.

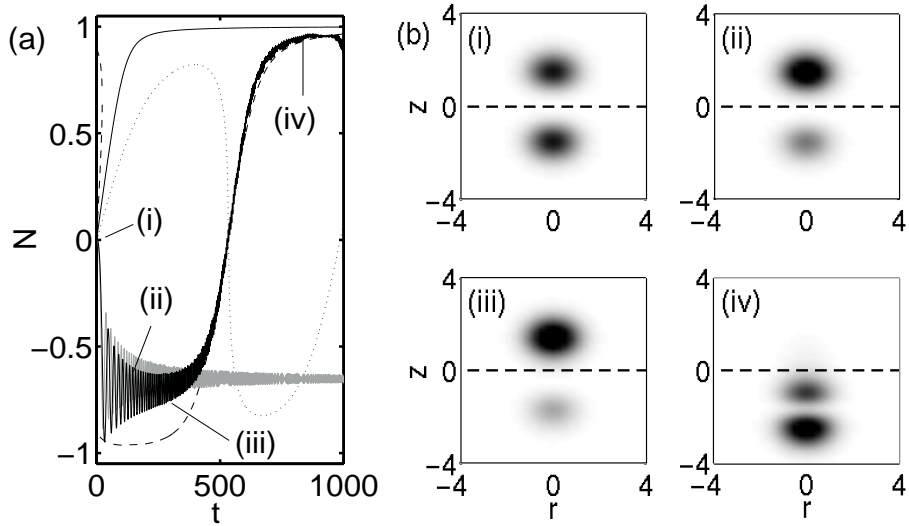


Figure 3. (a) Evolution of fractional population difference N as a function of time t , for a system initially prepared in state $|e\rangle$ based on the Gross-Pitaevskii equation (black line) and the two-state model (grey line) with initial condition $N(0) = 0$ and $\langle 0 | = 0$ and parameters $E_J = 0.10$, $E_C = 0.22$ and $2a = 3.77$ (obtained from the numerical solution of the GP equation). The fractional population differences for the eigenstates are also plotted for the ground (solid line), first excited (dashed line) and second excited states (dotted line). Here $h = 4h_1$, $\omega = 1$, $g = 10$ and the potential gradient $\dot{V} = R t$ increases at constant rate $R = 10^{-3} (h_1^2/a)$. (b) Snapshots of the evolution of the density distribution for case (a) when (i) $t = 0$, (ii) 100, (iii) 300 and (iv) 800 in units of (h_1^2/a) . The population of both wells is initially equal ($t = 0$). As the gradient is increased in (ii), (iii), population starts being transferred towards the right ($z > 0$), upper well. Increasing the asymmetry beyond a threshold value leads the population to be once again transferred to the left ($z < 0$), lower well. Eventually, (iv), a transition to the second excited state occurs (d) (see movie).

$g = 10$), leads to a reduction of the average population imbalance induced by the applied potential gradient of slightly more than a factor of 2. It is thus natural to ask if other factors (e.g. modifying initial trap aspect ratio, or changing barrier height h) will have the opposite effect. Tunneling has been predicted to be enhanced for 'pancake' traps ($\omega_z > 1$) [28], with such traps leading to a slightly increased current flow. Furthermore, such geometries feature enhanced energy splitting between ground and first excited state, thus making them more robust to coupling due to external (e.g. thermal [21, 43, 24]) perturbations. However, the suppression of tunneling induced by increased nonlinearities cannot be compensated by changing the geometry. We should further comment on the extent to which the above findings depend on the rate R with which the linear potential gradient $\dot{V} = R t$ is applied. Fig. 3(a) shows the dependence for $R = 10^{-3} (h_1^2/a)$. If one increases R by a factor of 10 then the maximum flow to the right well is reduced by roughly a factor of 2. Also flow to higher potential region can only be observed for approximately one tenth of the time, unless the gradient is ramped up to a particular value and subsequently kept constant. If the gradient is kept constant at the point of maximum population difference, the population remains

trapped in the right upper well, i.e. macroscopic quantum self-trapping [16,17,18,44] occurs to a state with higher potential energy. In this regime, where the gradient does not exceed the value at which the flow is reversed, the two-state model predicts the behaviour correctly.

4. Experimental Considerations

We now discuss the feasibility of observing flow to the upper well using phase imprinting [45]. Starting from the condensate ground state in a harmonic trap, population can be transferred to the excited states by applying a light-induced potential of the form

$$V_r(z; t) = \sin(\omega_0 t) \tanh(z) \quad (4)$$

for $(t < 0)$, where ω_0 and ϕ_0 are constants which we vary. At $t = 0$, the potential V_r is suddenly switched on such that there is a phase shift between the two wells. This simple phase-imprinting method does not distinguish between states with similar density and phase profiles such as ϕ_e , or ϕ . Other more sophisticated methods of preparing the initial state such as 2-photon adiabatic passage [46] could also be explored. However, as shown earlier in Fig. 2(b), the addition of the potential gradient allows us to distinguish between ϕ_e and ϕ .

We choose the phase-imprinting parameters such that the amplitude of the subsequent number oscillations between the wells in a symmetric double-well potential (i.e. in the absence of a potential gradient) are minimized. The time dynamics for this case are shown by the grey lines in Fig. 4, and essentially correspond to the ϕ -oscillations with $\hbar N(t) \neq 0$ discussed in [19,17,18,20,33]. For an imprinted phase of ϕ , most of the population is on the left well (grey line in Fig. 4(a)), while an imprinted phase of ϕ_e has population contained in the right well (grey line in Fig. 4(b)). In both cases, the addition of the potential gradient (solid lines) induces a flow to the right or upper potential well. Even at the time in the ϕ -oscillations cycle where most of the population is already on the right well and would subsequently flow back to the left, the addition of the gradient induces more flow to the right, as shown in Fig. 4(b). Note that, in this case, the population remains trapped in the right well until the influence of the second excited state becomes important (Fig. 3). If the correct initial state parameters are obtained from the full GP calculation, then the results shown in Fig. 4 can be reproduced using the two-state model, except for the transition to the second excited state. However, a full potential calculation is required to correctly predict the initial state and the dynamics for larger potential gradients, when the two-state model breaks down.

Finally, we discuss typical experimental parameters required for the demonstration of Josephson flow to the upper potential well. The number of atoms is given by

$$N = \frac{g}{4} \frac{a_2}{a} = \frac{g}{4} a \frac{h}{m!} : \quad (5)$$

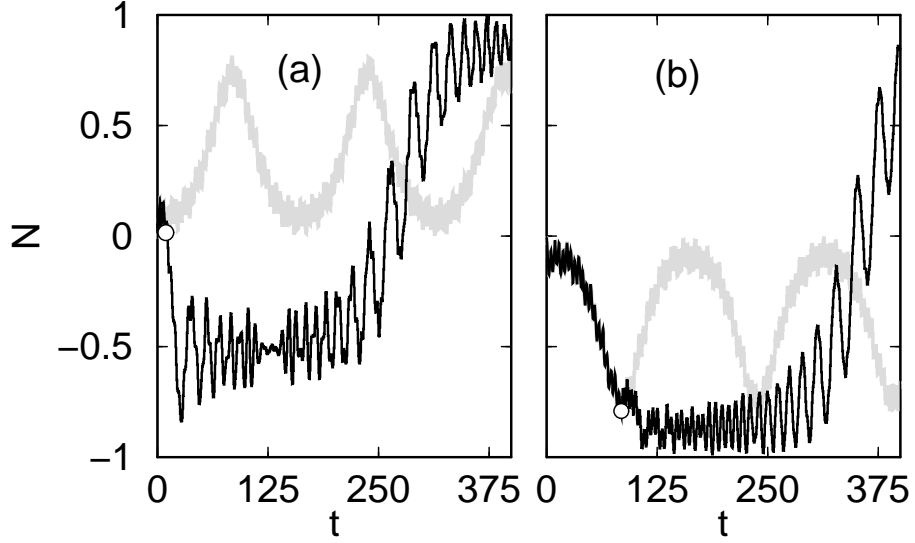


Figure 4. Evolution of fractional population difference N as a function of time for initial states prepared by phase imprinting ($j = h!_j$, $0 = 3!_0$). The grey and black curves correspond respectively to the absence of a potential gradient (i.e. symmetric double well), and the addition of a potential gradient $\Delta = R(t - t_1)$ increased linearly at rate $R = 2 \times 10^{-3} (\hbar!_j^2/a_j)$ from time t_1 , with this time indicated by the open circles. (a) $\Delta = h!_j$, $t_1 = 10!_j$ and (b) $\Delta = h!_j$, $t_1 = 85!_j$. Other parameters as in Fig. 2.

Therefore, for given dimensionless nonlinearity g , large atom numbers can be obtained for light, weakly-interacting, transversally weakly-confined systems. Note also that the total atom number is independent of the trap aspect ratio, as this cancels out for fixed g . For a large number of atoms, one should preferably choose species with a small value of $\frac{P}{m}$. For example, taking $g = 4$ and $!_j = 2 - 5$ Hz, we find: $N = 3300$ (^{23}Na) and 1000 (^{87}Rb). This number could be enhanced by a factor of 5 when using a larger nonlinearity which still exhibits this phenomenon, and $!_j = 2 - 1$ Hz, whereas further enhancement by a factor of 10 may be possible by tuning around a Feshbach resonance (e.g. ^{23}Na , ^{85}Rb , ^{133}Cs) [47]. In the case of ^7Li and ^{85}Rb , the number of atoms needed to observe such Josephson flow is not likely to exceed the critical value for collapse [48].

Note that for fixed, reasonably small, nonlinearity ($g < 10$), such that the effect can be clearly observed, one needs weak transverse confinement $!_j$ in order to obtain a reasonable number of atoms which can be imaged easily. However, small $!_j$ imply long time scales, such that the observation of this effect becomes limited by other factors (e.g. thermal damping [21,24,43], atom losses [42], etc.). If we choose $!_j = 2 - 5 - 100$ Hz, then the preparation of the $|e\rangle$ state requires a time $t_0 = (300 - 150)$ ms. and an applied field gradient $R = (10^{-3} - 10^{-2}) (\hbar!_j/a_j)$ (which translates into a Zeeman shift of $(1 - 100)$ MHz/cm) ramped up over a time $t_{\text{exp}} = (1.5 - 75)$ ms.

5. Conclusions

We have studied the Josephson dynamics of phase-imprinted condensates in a double-well potential in the presence of a time-dependent potential gradient. Preparation of a system with a phase slip across the weak link, leads to flow in a direction opposite to that of an initial ground state condensate. We have discussed the range of typical parameters for optimum experimental demonstration of this effect. This effect was found to be only weakly-dependent on sign of the scattering length, and on aspect ratio of the harmonic trap. However, suppression of this effect for large nonlinearities, tends to restrict the systems for which this effect can be observed to a few thousand atoms. An attractive candidate for the observation of the flow reversal is the recently realized atom chips [49] with a blue detuned laser beam to create the weak link. We believe that observation of the flow of phase imprinted states would provide a clear experimental demonstration of the Josephson effect.

Acknowledgments

We acknowledge funding from the U.K. EPSRC.

- [1] Likharev 1979 Rev. Mod. Phys. 51 101
- [2] D avis J C and Packard R E 2002 Rev. Mod. Phys. 74 741
- [3] B. D. Josephson, Phys. Rev. Lett. 1, 251 (1962)
- [4] Barone A and Paterno G Physics and Applications of the Josephson Effect (Wiley, New York, 1982).
- [5] Sukhatme K, Mukharsky Yu, Chul T and Pearson D 2001 Nature 411 280
- [6] Avendano and Varoquaux E 1988 Phys. Rev. Lett. 60 416
Pereverzev S V, Loshak A, Backhaus S, D avis J C and Packard R E 1997 Nature 388 449
Backhaus S, Pereverzev S V, Loshak A, D avis J C and Packard R E 1997 Science 278 1435.
- [7] M. H. Anderson et al. 1995 Science 269 198
D avis K B et al 1995 Phys. Rev. Lett. 75 3969
Bradley C C et al 1997 Phys. Rev. Lett. 75 1687
Bradley C C et al 1997 Phys. Rev. Lett. 79 1170
Fried D G et al. 1998 Phys. Rev. Lett. 81 3811
Robert A et al. 2001 Science 292 461
Dos Santos F P et al. 2001 Phys. Rev. Lett. 86 3459
Yosuke T, Makikawa K, Komori K, Takano T, Honda K, Kumakura M, Yabuzaki T and Takahashi Y 2003 Phys. Rev. Lett. 91 040404
- [8] Andrews M R, Townsend C G, Miesner H J, Durfee D S, Kum D M and Ketterle W 1997 Science 275 637
- [9] Shin Y, Leanhardt A E, Saba M, Pasquini T, Ketterle W and Pritchard D E 2003 Nature (subm.)
- [10] Tiecke T G, Kemann M, Buggle Ch, Shvarchuck I, von Klitzing W and Walraven J T M 2003 J. Opt. B: Quantum Semiclass. Opt. 5 S119
- [11] Anderson B P and Kasevich M A 1998 Science 282 1686
Orzel C, Tuchman A K, Fenselau M L, Yasuda M and Kasevich M A 2001 Science 291 2386
- [12] Cataliotti S, Burger S, Fort C, Maddaloni P, Minardi F, Trombettoni A, Serzini A, and Inguscio M 2001 Science 293 843

[13] Denschlag J H , Sim sarian J E , Ha ner H , M cKenzie C , B rowaeys A , Cho D , Helmerson K , Rolston S L and Phillips W D 2002 *J. Phys. B: At. Mol. Opt. Phys.* 35 3095

[14] Greiner M , Mandel O , Esslinger T , Hansch T W and Bloch I 2002 *Nature* 415 39

[15] Jack M W , Collett M J and Walls D F 1996 *Phys. Rev. A* 54 R 4625

[16] Milburn G J , Comey J , Wright E M and Walls D F 1997 *Phys. Rev. A* 55 4318

[17] Smerzi A , Fantoni S , Giovanazzi S and Shenoy S R 1997 *Phys. Rev. Lett.* 79 4950

[18] Raghavan S , Smerzi A , Fantoni S , and Shenoy S R 1999 *Phys. Rev. A* 59 620

[19] Marino I , Raghavan S , Fantoni S , Shenoy S R and Smerzi A 1999 *Phys. Rev. A* 60 487

[20] Raghavan S , Smerzi A and Kenkre V M 1999 *Phys. Rev. A* 60 R1787

[21] Zapata I , Sols F and Leggett A 1998 *Phys. Rev. A* 57 R28

[22] Javaneinen J and Ivanov M Yu 1999 *Phys. Rev. A* 60 2351

[23] Wu B and Niu Q 2000 *Phys. Rev. A* 61 023402

[24] Ruostekoski J and Walls D F 1998 *Phys. Rev. A* 58 R50

[25] Williams J , Walser R , Cooper J , Comell E and Holland M 1999 *Phys. Rev. A* 59 , R31

[26] Salasnich L , Parola A and Reatto L 1999 *Phys. Rev. A* 60 4171

[27] Zobay O , Garraway B M 2000 *Phys. Rev. A* 61 33603

[28] Williams J 2001 *Phys. Rev. A* 64 013610

[29] Giovanazzi S , Smerzi A and Fantoni S 2000 *Phys. Rev. Lett.* 84 4521

[30] Menotti C , Anglin J R , Cirac J I and Zoller P 2001 *Phys. Rev. A* 63 023601

[31] Sakellari E , Leadbeater M , Kylstra N J and Adams C S 2002 *Phys. Rev. A* 66 033612

[32] Leggett A J and Sols F 1991 *Found Phys* 21 353

[33] Anglin J R , Drummond P and Smerzi A 2001 *Phys. Rev. A* 64 063605

[34] Zhou Y , Zhai H , Lu R , Xu Z and Chang L 2003 *Phys. Rev. A* 67 043606
Li W -D , Zhang Yu and Liang J-Q 2003 *Phys. Rev. A* 67 065601

[35] Bulaevskii L N , Kuzii V V and Sobyanin A A 1977 *JETP Lett.* 25 290
Geshkenbeim V B , Larkin A I and Barone A 1987 *Phys. Rev. B* 36 235
Phys. Rev. Lett. 86 2427

[36] Baselmans J J A , Morpurgo A F , van Wees B J and Kapteijn T M 1999 *Nature* 397 43

[37] Baselmans J J A , van Wees B J and Kapteijn T M 2001 *Appl. Phys. Lett.* 79 2940

[38] Smilde H J H , Ariand , Blank D H A , Gerritsma G J , Hilgenkamp H and Rogalla H 2002 *Phys. Rev. Lett.* 88 057004

[39] Pu H , Baksmaty L O , Zhang W , Bigelow N P and Meystre P 2003 *Phys. Rev. A* 67 043605

[40] Backhaus S , Pereverzev S , Simmonds R W , Loshak A , Davis J C and Packard R E 1998 *Nature* 392 687

[41] Wu B , Diener R B and Niu Q 2002 *Phys. Rev. A* 65 025601
Diakonov D , Jensen L M , Pethick C J and Smith H 2002 *Phys. Rev. A* 66 013604
Mueller E J 2002 *Phys. Rev. A* 66 063603

[42] Kohler S and Sols F 2002 *Phys. Rev. Lett.* 89 60403

[43] Kohler S and Sols F 2003 *New J. Phys.* 5 94

[44] Ostromskaya E A et al. 2000 *Phys. Rev. A* . 61 013601 (R)

[45] Burger S et al. 1999 *Phys. Rev. Lett.* 83 5198
Denschlag J et al. 2000 *Science* 287 97

[46] Williams J E and Holland M J 1999 *Nature* 401 568

[47] Inouye S , Andrews M R , Stenger J , Miesner H -J , Stamm K um D M and Ketterle W 1998 *Nature* 392 151
Roberts J L , Claussen N R , Cornish S L and Wieman C E 2000 *Phys. Rev. Lett.* 85 728
Robert A et al. 2001 *Science* 292 461

[48] Bradley C C , Sackett C A and Hulet R G 1997 *Phys. Rev. Lett.* 78 985

[49] Ott H , Fortagh J , Schlotterbeck G , Grossmann A and Zimmermann C 2001 *Phys. Rev. Lett.* 87 230401
Hansel W , Hommelho P , Hansch T W and Reichel J 2001 *Nature* 413 498

Schneider S, Kasper A, vom Hagen Ch, Bartenstein M, Engeser B, Schumm T, Bar-Joseph I, Folman R, Feenstra L and Schieler J 2003 Phys. Rev. A 67 023612
Jones M P A et al. 2003 Phys. Rev. Lett. 91 080401